Robust future precipitation declines in CMIP5 largely reflect the poleward expansion of model subtropical dry zones

Jack Scheff[1] and Dargan M. W. Frierson[1]

Received 28 June 2012; revised 8 August 2012; accepted 10 August 2012; published 21 September 2012.

[1] Robust subtropical precipitation declines have been a prominent feature of general circulation model (GCM) responses to future greenhouse warming. Recent work by the authors showed that for the models making up the Coupled Model Intercomparison Project phase 3 (CMIP3), this drying was found mainly in the midlatitude-driven precipitation poleward of the model subtropical precipitation minima. Here, using more comprehensive diagnostics, we extend that work to 36 new CMIP5 models, and find that CMIP5 robust precipitation declines are also found mainly between subtropical minima and midlatitude precipitation maxima, implicating dynamic poleward expansion of dry zones rather than thermodynamic amplification of dry-wet contrasts. We also give the full seasonal cycle of these projected declines, showing that they are much more widespread in local spring than in local fall, and that for most of the year in the Northern Hemisphere they are entirely confined to the Atlantic side of the globe. **Citation:** Scheff, J., and D. M. W. Frierson (2012), Robust future precipitation declines in CMIP5 largely reflect the poleward expansion of model subtropical dry zones, *Geophys. Res. Lett.*, *39*, L18704, doi:10.1029/2012GL052910.

1. Introduction

[2] Since at least the middle of the last decade, it has been noted that most general circulation models (GCMs) agree on certain aspects of the large-scale precipitation (P) response to strong greenhouse-driven global warming [e.g., *Meehl et al.*, 2007b; *Held and Soden*, 2006; *McSweeney and Jones*, 2012]. These robust responses include increases in much of the high latitudes and parts of the deep tropics; and decreases in large areas of the subtropics, which have elicited particular concern [e.g., *Seager et al.*, 2007; *Hansen et al.*, 2008; *Frederiksen et al.*, 2011].

[3] Two distinct causes have been identified for the subtropical P decreases, at least in the models of the Coupled Model Intercomparison Project (CMIP) phase 3 (CMIP3) multimodel archive [*Meehl et al.*, 2007a]. *Held and Soden* [2006], as well as *Seager et al.* [2010] showed amplification of the multimodel-mean field of precipitation minus actual evaporation (P-E), with positive P-E regions becoming more positive, and negative P-E regions (i.e. subtropical oceans) becoming more negative, as a simple consequence of the Clausius-Clapeyron increase in vapor transport in a warmer future world [e.g., *Manabe and Wetherald*, 1975]. *Held and Soden* [2006] argued that these P-E changes are largely accomplished by P changes. Thus, all else equal, they suggest that models will tend to reduce P wherever $P < E$, including the subtropical dry margins of both the tropical wet belt and of the midlatitude storm tracks.

[4] Meanwhile, a number of studies [e.g., *Yin*, 2005; *Lorenz and DeWeaver*, 2007; *Lu et al.*, 2007; *Previdi and Liepert*, 2007; *Frederiksen et al.*, 2011] noted that in almost every CMIP3 model, the midlatitude storm tracks, baroclinic zones, and jets shift poleward with 21st-century greenhouse warming, and the subtropical dry zones and descending Hadley-Ferrel branches expand poleward in their wake. In contrast to the above mechanism, this less well understood dynamical response should mainly act to reduce P poleward of the subtropical P minima (potentially including wet regions as well as dry), and not on the dry margins of the tropical wet belt.

[5] In *Scheff and Frierson* [2012] (hereinafter SF12), the present authors showed that the robust future P reductions in the CMIP3 model subtropics are almost entirely located in midlatitude-driven P poleward of the model P minima, suggesting that their main cause is this poleward expansion of the dry zones, and not the thermodynamic "dry-get-drier" mechanism described above. In the present study, we extend the SF12 methods and results to 36 new models in the CMIP phase 5 multimodel archive [*Taylor et al.*, 2012] (listed in Table 1), further clarify the seasonal, hemispheric and regional variation in the results, and note some of the few differences between CMIP5 and CMIP3.

2. Results

2.1. All Models on the Same Grid

[6] Figure 1 depicts, for each point on a common ¼ × ¼ degree grid, the multimodel statistics of the 21st-century (1980–2099) trends of seasonal P in the native model gridboxes containing that point. All trends and significances are defined as in SF12, but using the CMIP5 scenarios "historical" and "rcp8.5". As shown in the legend, bold blue colors mean that almost all 36 CMIP5 models in Table 1 significantly increase P, bold red colors mean that almost all models significantly decrease P, and very light or white colors mean that few or no models have a significant trend in P. In contrast, pastel (and/or purple) hues represent disagreement within CMIP5 on the presence (and/or sign) of a significant model-gridbox-scale P response. The multimodel-mean late 20th-century (1980–1999) P climatology (computed as in SF12) is plotted as a reference, with thicker black contours corresponding to higher values of seasonal climatological P.

[1]Department of Atmospheric Sciences, University of Washington, Seattle, Washington, USA.

Corresponding author: J. Scheff, Department of Atmospheric Sciences, University of Washington, Box 351640, Seattle, WA 98195-1640, USA. (jscheff@uw.edu)

0094-8276/12/2012GL052910

Table 1. List of CMIP5 Models Analyzed in This Study

Model Name	Modeling Group
ACCESS1.0, ACCESS1.3	Commonwealth Scientific and Industrial Research Organization (CSIRO) and Bureau of Meteorology (BOM), Australia
BCC-CSM1.1, BCC- CSM1.1-M	Beijing Climate Center, China Meteorological Administration
BNU-ESM	College of Global Change and Earth System Science, Beijing Normal University
CanESM2	Canadian Centre for Climate Modelling and Analysis
CCSM4	National Center for Atmospheric Research, USA
CESM1(BGC), CESM1(CAM5)[a], CESM1(WACCM)[b]	Community Earth System Model Contributors, USA
CMCC-CM, CMCC-CMS	Centro Euro-Mediterraneo per i Cambiamenti Climatici, Italy
CNRM-CM5	Centre National de Recherches Météorologiques / Centre Européen de Recherche et Formation Avancées en Calcul Scientifique, France
CSIRO-Mk3.6.0	Commonwealth Scientific and Industrial Research Organization / Queensland Climate Change Centre of Excellence, Australia
FGOALS-g2	LASG, Institute of Atmospheric Physics, Chinese Academy of Sciences and CESS, Tsinghua University
FGOALS-s2	LASG, Institute of Atmospheric Physics, Chinese Academy of Sciences
FIO-ESM	The First Institute of Oceanography, SOA, China
GFDL-CM3, GFDL-ESM2G, GFDL-ESM2M	NOAA Geophysical Fluid Dynamics Laboratory, USA
GISS-E2-R	NASA Goddard Institute for Space Studies, USA
HadGEM2-AO	National Institute of Meteorological Research/Korea Meteorological Administration
HadGEM2-CC, HadGEM2-ES	Met Office Hadley Centre, United Kingdom
INM-CM4	Institute for Numerical Mathematics, Russia
IPSL-CM5A-LR, IPSL-CM5A-MR, IPSL-CM5B-LR	Institut Pierre-Simon Laplace, France
MIROC-ESM, MIROC-ESM-CHEM, MIROC5	Japan Agency for Marine-Earth Science and Technology, Atmosphere and Ocean Research Institute (The University of Tokyo), and National Institute for Environmental Studies
MPI-ESM-LR, MPI-ESM-MR	Max Planck Institute for Meteorology, Germany
MRI-CGCM3	Meteorological Research Institute, Japan
NorESM1-M, NorESM1-ME	Norwegian Climate Centre

[a]The rcp8.5 run 1 was branched from historical run 3, so for historical output only run 3 was used, rather than run 1 as specified in SF12.
[b]Run 1 was not fully available at the time of revision, so run 2 was used instead for both historical and rcp8.5.

[7] The CMIP5 seasonal P responses feature robust increases throughout almost all of the higher latitudes and in certain parts of the wet tropics, with robust declines in large portions of the subtropics, as in the CMIP3 work cited in section 1. Furthermore, the declines (bold red) are largely found in regions of baroclinically forced P, between the multimodel subtropical P minima and midlatitude P maxima. This is just what SF12 found for CMIP3, reinforcing the conclusion that these P decreases mainly reflect the poleward expansion of the seasonal model dry zones toward the midlatitudes. If anything, the declines tend to be even more robust in CMIP5 than in CMIP3, especially in the Southern Hemisphere in winter and spring (Figures 1c and 1d), though it is not clear whether this and other inter-CMIP differences stem from model or scenario differences. The equivalent plots for the 19 CMIP3 models examined in SF12 (scenario "A2") are presented as Figure S1 in the auxiliary material.[1]

[8] In contrast, the central, lowest-P portions of the subtropical dry zones tend to be mottled with various lighter shades in Figure 1, implying a lack of robustness in P response. Meanwhile, the tropical dry margins further equatorward show all sorts of responses, from robust drying (e.g., north of the east Pacific ITCZ in spring, Figure 1b) to robust wetting (e.g., in the Horn of Africa north of the ITCZ in boreal winter, Figure 1a) to robust insignificance (e.g., south of the Indian Ocean ITCZ in winter, Figure 1c), and everything in between. Thus, the simple "dry-get-drier" rule from the amplified vapor transport does not appear to be in phase with the CMIP5 P responses. Instead, the dynamical replacement of midlatitude wetness with subtropical dryness and descent offers a much cleaner explanation for the robust subtropical P declines, as in SF12.

[9] Furthermore, and also as in SF12, the high-latitude robust wetting in Figure 1 is often located directly across the climatological midlatitude wet belt from the subtropical robust drying (e.g., throughout the Southern Hemisphere in all seasons, or in the north Pacific in winter), so that the robust P response pattern is in near-quadrature with the multimodel climatology in the extratropics. This phase relationship suggests a poleward shift of certain midlatitude storm tracks as a key element of P changes in CMIP5.

[10] This general pattern does have some local exceptions, many of which are more robust in CMIP5 (Figure 1) than in CMIP3 (Figure S1). Notably, the region north of the ITCZ in the American sector often features robust P decreases that fully straddle the subtropical dry belt (e.g., the western subtropical north Atlantic in winter, or the Caribbean in summer.) The Southern Hemisphere in springtime (Figure 1d) sees some similar "dry-get-drier" robust decreases as well, most notably in southern Africa. However, the overall impression remains that subtropical P declines in CMIP5, as in CMIP3, are dominant *poleward* of the driest zones, i.e. in regions of extratropically forced P. In fact, many of the above exceptions are situated at regional saddles in the P field, where midlatitude and tropical P zones appear to connect or overlap, so that they might also be conceivably driven by the poleward retreat of extratropical dynamic P forcing. *Tyson and Preston-Whyte* [2000] details the frontal production of springtime southern-African P in particular.

[11] Interestingly, there is also a pronounced spring-fall asymmetry (compare Figures 1b and 1d) in both hemispheres, with drying (of both types) more prevalent in local spring. This was already noted broadly for CMIP3 by

[1]Auxiliary materials are available in the HTML. doi:10.1029/2012GL052910.

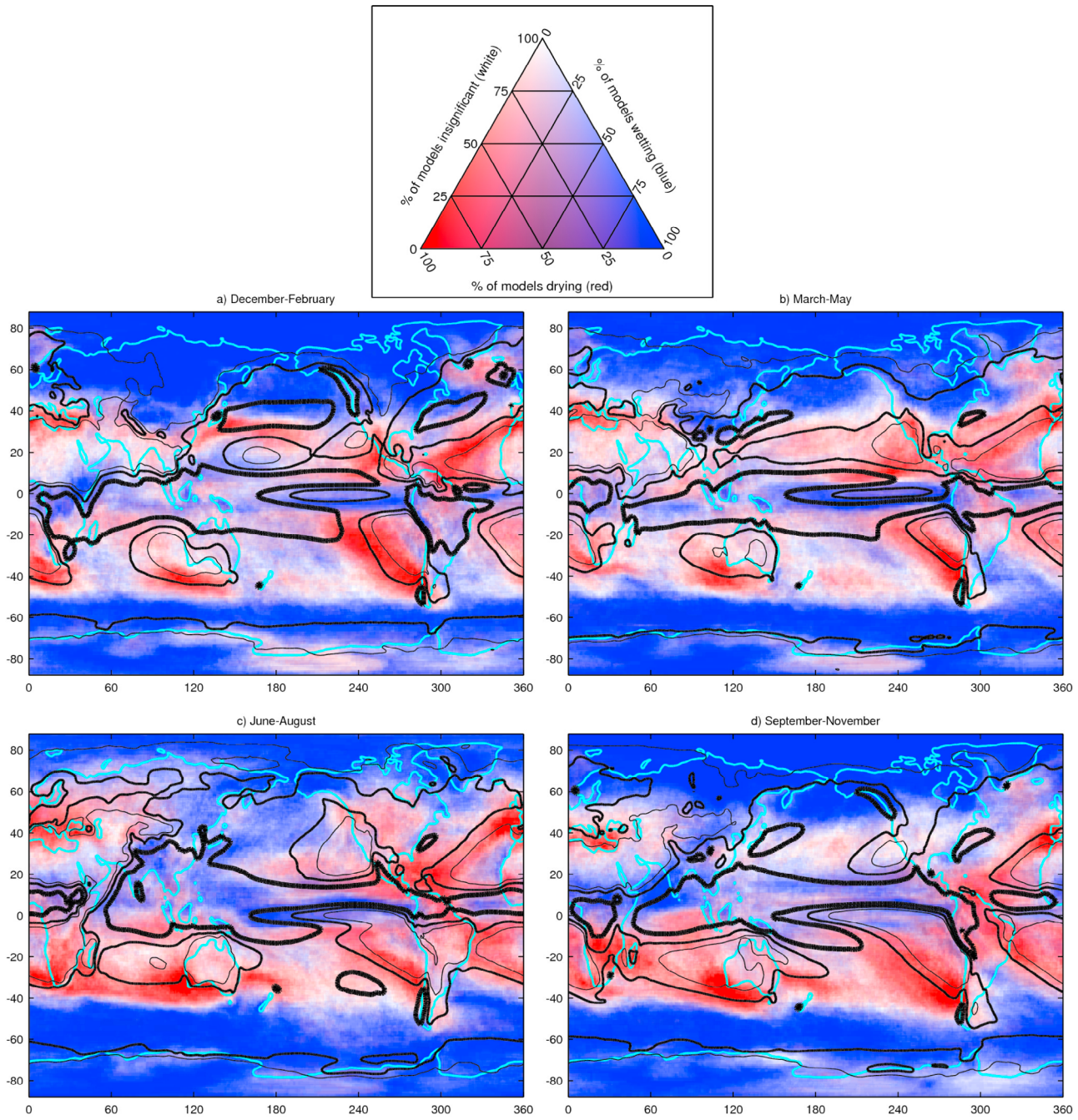

Figure 1. (a–d) In each season, black contours are the 1980–1999 CMIP5 multimodel climatological P (1,2,5 mm/day lightest to boldest.) At each point, the colored shading shows the proportion of CMIP5 models for which the rcp8.5 1980–2099 seasonal P trend in the native model gridbox containing that point is negative and significant (red), positive and significant (blue), or insignificant (white), according to the legend.

Biasutti and Sobel [2009] and specifically for the monsoon regions by *Seth et al.* [2011] for CMIP3 and by *Seth et al.* [2012] for CMIP5; however Figure 1 makes it clear that this is a robust phenomenon extending across much of the subtropics and midlatitudes. The reason for this consistent asymmetry is unclear, since the *Seth et al.* explanation of reduced low-level moisture supply at the end of a warmer future dry season is only applicable over land. However, it is still a noticeable pattern that demands explanation.

2.2. Model-by-Model Approach

[12] The above interpretation using the multimodel climatology as a reference may be misleading for individual, biased models, because their own climatological dry and wet zones may be located in different latitudes than those of the ensemble mean. In SF12, we introduced a novel system for recording each CMIP3 model's seasonal P response pattern relative to the pattern of its *own* climatology in a uniform fashion that can be collated across many models.

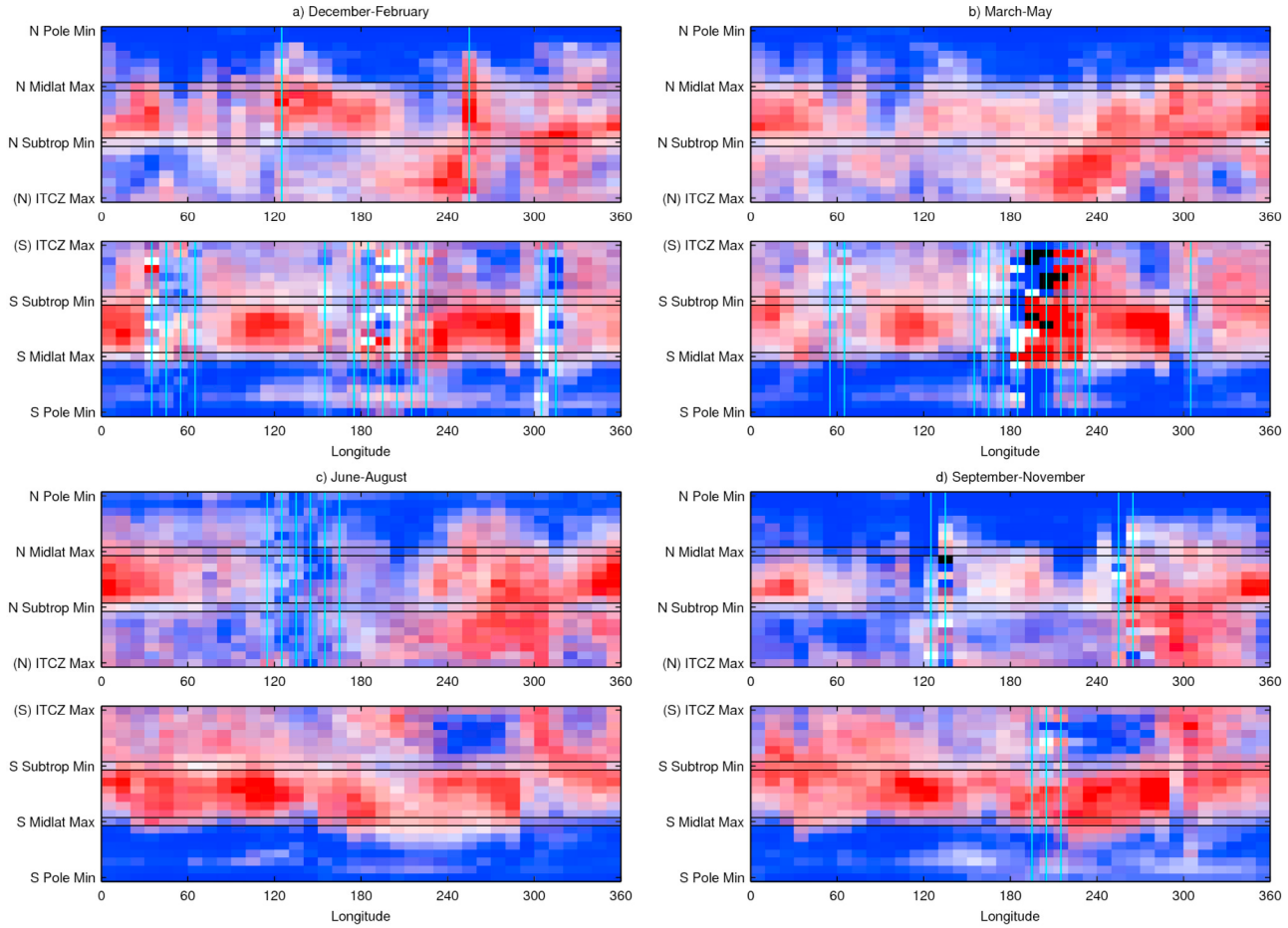

Figure 2. (a–d) For each season, 10°-wide longitude band, and meridional "location" relative to the individual models' 1980–1999 climatological P features, the colored shading gives the CMIP5 multimodel average frequencies of negative-and-significant (red), positive-and-significant (blue), and insignificant (white) rcp8.5 1980–2099 P trends in the individual model latitudes corresponding to that "location". The color values are exactly as in Figure 1. Longitude bands for which fewer than half of the models possess these climatological P features, and thus fewer than half of the models contribute to the plotted values, are struck through in cyan as a warning. For more detailed information, see the appendix, and see *Scheff and Frierson* [2012].

[13] In Figure 2, we apply this method to the CMIP5 models to confirm the results in section 2.1. In each seasonal panel of Figure 2, the horizontal axis marks off thirty-six 10°-longitude-wide bands, zonally spanning the globe. Each band supports a vertical column of boxes colored as in Figure 1, stretching from "South Pole Min" up to "North Pole Min", and interrupted at the ITCZ(s) for visual clarity. As in Figure 1, the colors indicate how many models have significantly increasing, significantly decreasing, or insignificant 21st-century P trends.

[14] The key aspect of this method is that in each of these columns, the correspondence between the vertical "coordinate" and actual local latitude is determined *separately* for *each model*, using that model's own late-20th-century P climatology. Thus, for example, the bluish color in Figure 2a in the leftmost longitude band at the north midlatitude maximum means that many individual CMIP5 models respond to rcp8.5 with significant December–February 0–10°E P increases at the latitude of *their* present-day December–February 0–10°E north midlatitude P maximum, *whatever that latitude is for each model.* For more details, see Appendix A, and/or SF12.

[15] As in SF12, the pattern is broadly similar to that found with the fixed-grid approach, but clearer, and more credible due to this spatial bias removal. In particular, the Southern Hemisphere of Figure 2 in each season strongly supports the conclusions from section 2.1, with the robust P reductions characterizing not the models' subtropical P minima and vicinity, but rather the broad belts between those minima and the midlatitude P maxima (including both dry and wet regions.) This is most remarkably so in summer and fall (Figures 2a and 2b) but still holds well in the other seasons, though the exception noted in section 2.1 near southern Africa (10°–50° longitude or so) in spring (Figure 2d) is still apparent.

[16] The meridional quadrature pattern noted in section 2.1, with bold blues located directly across the models' southern midlatitude P maxima from the bold reds, is perhaps even more striking in this view than in Figure 1, and again strongly suggests a poleward shift of southern midlatitude precipitation in all seasons in response to future greenhouse-driven warming in CMIP5. In contrast, the signals at and equatorward of the south subtropical minima are varied and usually non-robust, even in wet tropical zones near the (south) ITCZ.

In short, the Southern Hemisphere robust P response in this framework looks much more like dynamic poleward expansion of dryness into the midlatitudes than thermodynamic "dry-get-drier," just as in section 2.1 and in SF12.

[17] In the Northern Hemisphere, though, Figure 2 is more ambiguous. In each season, the Europe-Africa region (roughly 340°–050° longitude) responds just like the Southern Hemisphere above – the subtropical dry zones expand poleward without any robust drying in the tropical dry margins (or wet tropics). This also characterizes the northwest Pacific (130°–190°) in winter only (Figure 2a), and the north subtropical Atlantic (270°–340°) in spring only (Figure 2b). However, the American/Atlantic sector (roughly 210°–330°) always contains a similarly broad drying region centered on or equatorward of the P minimum. Meanwhile, through most of the year (Figures 2b–2d) the Asian continent and neighboring Pacific (50°–190°) don't show any robust P declines at all, in *any* feature-relative "location" (nor in any real location on Figures 1b–1d for that matter), subtropical or otherwise.

[18] So, in the Northern Hemisphere, which (if any) type of subtropical drying appears to dominate the CMIP5 responses is a strong and somewhat seasonally invariant function of longitude. This quasi-wavenumber-1 asymmetry was discussed briefly in section 2.1 above and in SF12, but this view makes it clearer. Poleward expansion is still the most common Northern Hemisphere drying type overall, but not near-universally as in the Southern Hemisphere.

[19] Figure 2 also reproduces the curious spring-fall asymmetry seen in Figure 1, especially in the Northern Hemisphere, where the extent of robust drying in local fall (Figure 2d) is strikingly low compared to the other seasons.

[20] Finally, the equivalent of Figure 2 for the SF12 CMIP3 models is provided as Figure S2 for comparison. The greater robustness of Southern Hemisphere winter-spring drying in CMIP5 than in CMIP3, noted for Figures 1 and S1, is reaffirmed. Similarly, the local robust "dry-get-drier" responses found in southern Africa (and parts of South America) in local spring and in the subtropical North Atlantic in local winter are largely *novel* features of CMIP5, as suggested in section 2.1. (Other CMIP5 "dry-get-drier" regions were robust in CMIP3, especially near the Americas north of the ITCZ(s) [SF12]).

3. Summary and Discussion

[21] In a previous study, the authors [SF12] used one established and one novel diagnostic method to argue that robust local precipitation (P) decline due to future greenhouse warming in 19 CMIP3 GCMs was largely an extratropical phenomenon, associated with the well-known poleward expansion of the individual GCMs' subtropical low-P zones. In section 2 above, the SF12 techniques were improved and extended to 36 new CMIP5 models, and the CMIP3 result was strongly reaffirmed. Aspects of the result's seasonal cycle involving local spring and fall (in addition to summer and winter) were clarified, and regional exceptions to the overall result were noted.

[22] It is instructive to consider why P declines roughly centered on the subtropical dry minima themselves ("dry-get-drier" decreases), expected from basic moist theory, are not more widespread. *Held and Soden* [2006], *Seager et al.* [2010], SF12, and others show that P-E does decrease in these regions in most CMIP3 models, and SF12 shows that this doesn't translate to robust P declines, implying a role for E increases in balancing the increased vapor flux divergence. Both of these properties can be confirmed in CMIP5 to some degree using the SF12 diagnostics (not shown.) However, *Seager et al.* [2010] show that P-E itself does not decrease so strongly on the tropical dry margins, due to the slowdown of the tropical circulation under global warming [e.g., *Vecchi and Soden*, 2007; *Held and Soden*, 2006]. Furthermore, *Neelin et al.* [2006] note the inconsistency of P response to global warming on the tropical dry margins, as different regions and models see the wet ITCZ either advance toward the subtropical dry region, or retreat away from it. Thus, it is plausible that the dry-get-drier mechanism is still working to reduce P, but that the above factors combine to cancel and/or overwhelm this signal in the lower-latitude portions of the dry subtropics, leaving the midlatitude flanks as the robust loci of thermodynamic P reduction. However, this still does not explain why the reductions often extend poleward all the way to the midlatitude wet maxima, with P increases situated poleward of the maxima (the shift-dominated pattern discussed in section 2). In any case, it seems simpler to describe the robust model P decreases as poleward retreat of some extratropically-driven P (affecting both present-day dry and wet regions) than as amplification of dry-wet contrasts.

Appendix A

[23] The precise meaning of the vertical axes in Figures 2 and S2 is as follows: for each model, in each season and each of the thirty-six 10°-longitude-wide bands, we use criteria defined in SF12 (with one minor difference, explained below) to identify the latitudes of the tropical ITCZ peak(s) and (if possible) the subtropical minima and midlatitude peaks of the 10°-zonal-mean late 20th century P. If these latter two features are present in either hemisphere, then every latitude between the pole and the (nearest) ITCZ is classified according to which two features it lies between, and then according to its 10°-zonal-mean late 20th century model P value relative to those two features. For example, all model latitudes lying between the model's 0–10°E December–February subtropical minimum and midlatitude maximum, and whose 0–10°E December–February P is between 2/6 and 3/6 of the way from the former to the latter, are binned together. In each such bin, we then note the fraction of latitudes for which the 21st-century trend in the model's 10°-zonal-mean P is significant and upward, and similar for insignificant and for significant and downward. For each model, these fractions are usually either zero or unity, since the bins usually contain latitudes that are close together and behave similarly.

[24] This entire procedure is then repeated separately for each model, and the above fractions are averaged across all applicable models at the same relative bin-definition (i.e. same vertical coordinate in Figures 2 and S2) to obtain the fractions color-plotted in Figures 2 and S2. Because the individual-model fractions are usually zero or unity, the averages can be thought of as the proportion of *models* that dry, wet, or leave P unchanged under rcp8.5 greenhouse warming in whichever individual-model latitudes are locally represented. For a more detailed version of these two paragraphs, see SF12.

[25] The small difference between the P feature definition criteria used here and those used in SF12, mentioned above, is as follows: for a given hemisphere (north or south), we now declare these features locally absent if the putative subtropical minimum falls poleward of 55° latitude, not 66.5°. This stricter criterion eliminates clear false positives in the warm season in the vicinity of far-eastern Siberia and the Sea of Okhotsk, and does not introduce any false negatives. (For features of the *P-E* field, we still recommend the original value of 66.5°.)

[26] **Acknowledgments.** The authors acknowledge the World Climate Research Programme's Working Group on Coupled Modelling, which is responsible for CMIP, and we thank the climate modeling groups listed in Table 1 for producing and making available their model output. For CMIP, the U.S. Department of Energy's Program for Climate Model Diagnosis and Intercomparison provides coordinating support and leads development of software infrastructure in partnership with the Global Organization for Earth System Science Portals. Also, the authors would like to thank M. Pritchard for graphical inspiration. This work is funded by NSF grants ATM-0846641 and ATM-0936059.

[27] The Editor thanks Timothy Merlis and an anonymous reviewer for their assistance in evaluating this paper.

References

Biasutti, M., and A. H. Sobel (2009), Delayed Sahel rainfall and global seasonal cycle in a warmer climate, *Geophys. Res. Lett.*, *36*, L23707, doi:10.1029/2009GL041303.

Frederiksen, C. S., J. S. Frederiksen, J. M. Sisson, and S. L. Osbrough (2011), Changes and projections in Australian winter rainfall and circulation: Anthropogenic forcing and internal variability, *Int. J. Clim. Change Impacts Responses*, *2*(3), 143–162.

Hansen, J., et al. (2008), Target atmospheric CO_2: Where should humanity aim?, *Open Atmos. Sci. J.*, *2*, 217–231, doi:10.2174/1874282300802010217.

Held, I., and B. Soden (2006), Robust responses of the hydrological cycle to global warming, *J. Clim.*, *19*, 5686–5699, doi:10.1175/JCLI3990.1.

Lorenz, D. J., and E. T. DeWeaver (2007), Tropopause height and zonal wind response to global warming in the IPCC scenario integrations, *J. Geophys. Res.*, *112*, D10119, doi:10.1029/2006JD008087.

Lu, J., G. A. Vecchi, and T. J. Reichler (2007), Expansion of the Hadley cell under global warming, *Geophys. Res. Lett.*, *34*, L06805, doi:10.1029/2006GL028443.

Manabe, S., and R. T. Wetherald (1975), The effects of doubling the CO_2 concentration on the climate of a general circulation model, *J. Atmos. Sci.*, *32*, 3–15, doi:10.1175/1520-0469(1975)032<0003:TEODTC>2.0.CO;2.

McSweeney, C., and R. Jones (2012), Consensus and confidence: Measuring, communicating and interpreting model ensemble agreement, paper presented at Workshop on CMIP5 Model Analysis, World Clim. Res. Programme, Honolulu, Hawaii.

Meehl, G. A., C. Covey, T. Delworth, M. Latif, B. McAvaney, J. F. B. Mitchell, R. J. Stouffer, and K. E. Taylor (2007a), The WCRP CMIP3 multi-model dataset: A new era in climate change research, *Bull. Am. Meteorol. Soc.*, *88*, 1383–1394, doi:10.1175/BAMS-88-9-1383.

Meehl, G. A., et al. (2007b), Global climate projections, in *Climate Change 2007: The Physical Science Basis*, edited by S. Solomon et al., pp. 747–845, Cambridge Univ. Press, Cambridge, U. K.

Neelin, J. D., M. Munnich, H. Su, J. E. Meyerson, and C. E. Holloway (2006), Tropical drying trends in global warming models and observations, *Proc. Natl. Acad. Sci. U. S. A.*, *103*, 6110–6115, doi:10.1073/pnas.0601798103.

Previdi, M., and B. G. Liepert (2007), Annular modes and Hadley cell expansion under global warming, *Geophys. Res. Lett.*, *34*, L22701, doi:10.1029/2007GL031243.

Scheff, J., and D. Frierson (2012), Twenty-first-century multimodel subtropical precipitation declines are mostly midlatitude shifts, *J. Clim.*, *25*, 4330–4347, doi:10.1175/JCLI-D-11-00393.1.

Seager, R., et al. (2007), Model projections of an imminent transition to a more arid climate in southwestern North America, *Science*, *316*, 1181–1184, doi:10.1126/science.1139601.

Seager, R., N. Naik, and G. A. Vecchi (2010), Thermodynamic and dynamic mechanisms for large-scale changes in the hydrological cycle in response to global warming, *J. Clim.*, *23*, 4651–4668, doi:10.1175/2010JCLI3655.1.

Seth, A., S. Rauscher, M. Rojas, S. Camargo, and A. Giannini (2011), Enhanced spring convective barrier for monsoons in a warmer world?, *Clim. Change Lett.*, *104*, 403–414, doi:10.1007/s10584-010-9973-8.

Seth, A., S. Rauscher, A. Giannini, S. Camargo, M. Biasutti, and M. Rojas (2012), Springtime drying in monsoon regions in a warmer world: A CMIP5 analysis of ESMs and CMs, paper presented at Workshop on CMIP5 Model Analysis, World Clim. Res. Programme, Honolulu, Hawaii.

Taylor, K. E., R. J. Stouffer, and G. A. Meehl (2012), An overview of CMIP5 and the experiment design, *Bull. Am. Meteorol. Soc.*, *93*, 485–498, doi:10.1175/BAMS-D-11-00094.1.

Tyson, P. D., and R. H. Preston-Whyte (2000), *The Weather and Climate of Southern Africa*, Oxford Univ. Press, Cape Town, South Africa.

Vecchi, G. A., and B. J. Soden (2007), Global warming and the weakening of the tropical circulation, *J. Clim.*, *20*, 4316–4340, doi:10.1175/JCLI4258.1.

Yin, J. (2005), A consistent poleward shift of the storm tracks in simulations of 21st century climate, *Geophys. Res. Lett.*, *32*, L18701, doi:10.1029/2005GL023684.